

Spectral Aspects of the Microwave Ionization of Atomic Rydberg States

Andreas Buchleitner and Dominique Delande

Laboratoire de Spectroscopie Hertzienne de l'Ecole Normale Supérieure
Tour 12, Etage 1, Université Pierre et Marie Curie
4, place Jussieu, F-75252 Paris Cedex 05, France.

Chaos, Solitons and Fractals, **5**, 1125 (1995)

Abstract

We perform a numerical study of the microwave ionization of a Rydberg state of atomic hydrogen, on the grounds of a one dimensional model of the atom. Our work unifies, for the first time, all the different approaches to the microwave problem realized up to date, additionally taking into account the coupling to the continuum. This allows for an unambiguous identification of structures in the level dynamics with the observed ionization probability, as well as for testing the correlation between the electronic density distribution and the lifetime of individual eigenstates. Special emphasis is given to the sensitivity of the quasienergy spectrum with respect to changes of an external parameter, which seems a good candidate for a general characterisation of quantal chaotic systems. The impact on experimental results is discussed, notably by stressing the important role of the experimental interaction time.

1 Introduction

Rydberg atoms exposed to intense, monochromatic fields are ideal candidates for the theoretical *and* experimental study of quantal systems which show nonlinear dynamics in their classical limit. They represent one of the three prototypes of such systems subject to current research in atomic physics. The best understood among these are today Rydberg states of hydrogen or alkalines exposed to strong, static magnetic or crossed magnetic and electric fields [1, 2], where, as in the microwave problem, the nonlinearity of the classical equations of motion depends continuously on the relative strength of the external perturbation with respect to

the corresponding atomic field. The third prototype to be mentioned in this context are doubly excited states of helium or other two-electron atoms [3], a system which is classically nonlinear without the need of any external perturbation.

Both Rydberg states in static fields or doubly excited states, are described by a time independent Hamiltonian. Energy is therefore a conserved quantity and the eigenstates of the quantum problem are stationary. The chaotic character of the dynamics expresses itself either in the exponential divergence of nearby trajectories or in the complicated exchange of energy between the different internal degrees of freedom of the atom (recall that chaos needs at least two degrees of freedom in a time-independent dynamical problem [4]), much as the (regular) energy exchange between two coupled oscillators. As the (time-resolved) level of excitation along the internal degrees of freedom of a microscopic object like the hydrogen atom is rather difficult to access, the underlying irregularity of the classical dynamics of such quantum objects is generally monitored and tested by their spectral properties, these latter allowing to account for the destabilisation of the dynamics by the proliferation of unstable periodic orbits which completely determine the dynamics in the regime of globally chaotic motion.

On the contrary, Rydberg atoms subjected to a coherent microwave field of angular frequency ω are described by a Hamiltonian which *does* explicitly depend on time, and the energy of the atomic electron is no more a conserved quantity. However, the total energy of the atom *together with the microwave field* is conserved, and one can map the time-dependent problem to a time-independent one by extending the classical phase space as well as the Hilbert space the quantum object is living in, by one more degree of freedom, the interaction time. The canonical conjugate of this additional “coordinate” is the energy of the atomic electron in the microwave field. Even if we restrict the atomic degrees of freedom to the one defined by the principal quantum number n_0 , the classical motion of the Rydberg electron in the periodic field becomes chaotic for values of the microwave amplitude F larger than a certain threshold value. In this system, it is the nonlinear coupling of the *one and only* atomic degree of freedom with the degree of freedom generated by the field, and best described by the number of photons exchanged between the atom and the microwave, which generates the irregularity of the classical dynamics. Since the energy of the atom (i. e. the population distribution over the unperturbed bound states n_0) is relatively easy to access in laboratory experiments, the microwave excitation and ionization of Rydberg states consequently provides the best object for testing the properties of quantal energy transport and transfer under the conditions of an underlying irregularity of the classical dynamics. The typical experimental approach consists in measuring the ionization probability of a Rydberg state exposed to a microwave field of defined frequency and amplitude [5, 6, 7], for a given interaction time, or in the analysis of the microwave-induced redistribution of the bound state population initially prepared in a well defined unperturbed atomic state [8, 9]. Both approaches are complementary in the sense that they probe rather global and/or

asymptotic properties of the quantum transport, in the former case, and rather local ones, in the latter. The ionization probability at a given interaction time convolutes all the detailed information about the excitation of the different atomic bound states during the ionization process and depends, for the typical time scales involved in our problem, essentially on the asymptotics of the electronic density of the atom. The analysis of the population distribution over the bound states of the atom rather aims at the transport in the vicinity of the initial state and at the impact of invariant structures of classical phase space on the quantum transport. The latter analysis is actually quite hard to realize in laboratory experiments, at least at a degree of resolution in the atomic degrees of freedom (principal and, eventually, angular momentum quantum number) which would allow for an even only qualitative comparison to local structures of classical phase space. However, it can be and has been performed in numerical experiments on the microwave ionization of a one dimensional model atom [10, 11, 12].

It is the purpose of the present paper to illustrate some of the asymptotic and local properties of quantal energy transport along the Rydberg series towards the continuum, for an underlying classical dynamics which is typically mixed regular and chaotic, depending on the choice of the initial conditions. The investigation of some properties of the quantum spectrum of our problem will especially allow us to separate the different time scales associated with the local and asymptotic features of quantum transport. Since the appearance of chaos in this system is essentially independent on taking into account or not the second atomic degree of freedom, i. e. the excitation along the angular coordinate, we will restrict ourselves to an extensive study of a one dimensional model atom. This model differs from the real object of laboratory experiments by the absence of the angular momentum quantum number ℓ . It has been shown elsewhere [13, 14, 15] that it provides a good approximation to the quantum dynamics of the real hydrogen atom in a microwave field, as long as the initial atomic state corresponds to a classical trajectory of sufficiently high eccentricity. All the conclusions we will draw throughout this paper are essentially unaffected by the modifications which are induced by the presence of one more degree of freedom in the real dynamics. These modifications will be the subject of another contribution [12, 16].

The paper is organized as follows: section 2 briefly recapitulates the theoretical basis of our approach (for details, see [17]). Section 3 illustrates the classical-quantum correspondence by a projection of some typical eigenstates of the microwave problem onto the classical phase space. We also give some indications on the correlation between the local and asymptotic properties of quantum transport. Section 4 introduces some quantities which are typically accessed in laboratory experiments, relates them to characteristic properties of the quantum spectrum and discusses their sensitivity towards changes of the parameters defining the physical situation, such as the principal quantum number of the initial state and the frequency of the driving field. Section 5 finally provides a discussion of the different time scales associated to the global and to the local properties

of the quantum spectrum and their experimental relevance. Section 6 concludes the paper.

2 Theoretical Foundations

Let us first supply some definitions and fundamental theoretical notions which will be necessary for the discussion of our numerical results in the following. Throughout this paper, we shall place ourselves in the reference frame defined by the center of mass of the electron and the atomic nucleus, neglect relativistic effects, and restrict ourselves to the case of linear polarization of the microwave field along the z -axis (since an oscillatory field of circular polarization implies largely regular classical dynamics [18, 19]). For the sake of comparison of our quantum results to the classical motion, we first treat briefly the classical motion.

2.1 Classical Dynamics

In the velocity gauge, the one dimensional Hamilton function H writes in atomic units:

$$H = \frac{p_z^2}{2} - \frac{F p_z \sin \omega t}{\omega} - \frac{1}{|z|} + \frac{F^2 \sin^2 \omega t}{2\omega^2}. \quad (1)$$

The last term in this equation is a constant operator and can be skipped: its mean value gives the “ponderomotive shift”, i. e. the mean energy of a free electron in an oscillating field of angular frequency ω and amplitude F .

Since all the terms in (1) appear as power functions of the position or of the momentum, the classical equations of motion do actually obey a scaling law and are invariant under a transformation which leaves the values of the “scaled variables”

$$\begin{cases} F_0 = n_0^4 F, \\ \omega_0 = n_0^3 \omega, \\ t_0 = n_0^{-3} t \end{cases} \quad (2)$$

unchanged, with n_0 the principal quantum number. F_0 , ω_0 and t_0 design, respectively, the scaled amplitude of the microwave, its scaled frequency, and the scaled interaction time during which the atoms are exposed to the radiation. The latter measures (up to a factor 2π) the interaction time in terms of the classical Kepler period of the unperturbed atomic electron on its n_0^{th} Bohr orbit. As the principal interest of the microwave problem resides in the comparison of the “true” quantum dynamics to the nonlinear classical one, most numerical or experimental data which can be found in the literature are presented in terms of these reduced variables.

Changing from cartesian to semi-parabolic coordinates

$$u = (2z)^{1/2}, \quad p_u = u p_z, \quad (3)$$

allows for a simple expression of the equations of motion which reduce to the ones of a harmonic oscillator (the frequency of which depends on n_0), in the absence of the microwave field. The action angle variables I and Θ of a harmonic oscillator are therefore well-suited for the representation of classical (and quantal) probability transport in the classical phase space. They follow from u and p_u according to [20]

$$\begin{cases} \frac{I}{\alpha} = \frac{1}{4} \left(\frac{u^2}{\alpha^2} + p_u^2 \right), \\ \Theta = 2 \arctan \frac{p_u \alpha}{u}, \end{cases} \quad (4)$$

where α denotes a scaling parameter [12, 20] which ensures the consistency of this definition with eq. (2). In the semiclassical limit, I corresponds to the principal quantum number n_0 which labels the bound states of the atom.

2.2 Quantum Dynamics

For the quantum treatment of our problem, we first take advantage of the time-periodicity (period $T = 2\pi/\omega$) of the Hamiltonian. This allows for the use of the Floquet theorem [21, 22, 23] which guarantees the existence of stationary solutions $|\psi_j(t)\rangle$, the ‘‘Floquet states’’, of the eigenvalue equation

$$\mathcal{H}|\psi_j(t)\rangle = \varepsilon_j|\psi_j(t)\rangle, \quad (5)$$

where \mathcal{H} designs the ‘‘Floquet Hamiltonian’’

$$\mathcal{H} = H - i \frac{\partial}{\partial t} = \frac{p_z^2}{2} - \frac{F p_z \sin \omega t}{\omega} - \frac{1}{|z|} - i \frac{\partial}{\partial t} \quad (6)$$

acting on the extended Hilbert space of time-periodic functions of period T . According to Floquet, any solution of the Schrödinger equation can be written as

$$|\psi(t)\rangle = \sum_j c_j \exp(-i\varepsilon_j t) |\psi_j(t)\rangle, \quad (7)$$

the eigenstates of (5) are a complete and orthogonal basis at any time t .

In order to obtain the lifetimes and thus the ionization rates of the different eigenstates of \mathcal{H} , we use the complex dilation technique, in the way it has been described in refs. [15, 17]. The dilated Floquet Hamiltonian writes then

$$\mathcal{H}_\theta = \frac{p_z^2 e^{-2i\theta}}{2} - \frac{F p_z e^{-i\theta} \sin \omega t}{\omega} - \frac{e^{-i\theta}}{|z|} - i \frac{\partial}{\partial t}. \quad (8)$$

Its eigenvalues and eigenvectors are

$$\mathcal{H}_\theta |\psi_{j\theta}\rangle = \varepsilon_{j\theta} |\psi_{j\theta}\rangle, \quad (9)$$

where the complex $\varepsilon_{j\theta}$ are actually independent of θ provided it has been chosen sufficiently large [24, 25]. The real part of $\varepsilon_{j\theta}$ just coincides with the energy of the resonance, and the modulus of its imaginary part gives half its width.

Once the eigenvalues and eigenvectors of \mathcal{H}_θ are obtained, the time evolution operator generated by H can be calculated [17]. This especially allows for the calculation of the ionisation probability P_{ion} of an initial (bound) state $|\Phi_0\rangle$ after an interaction time t ,

$$P_{\text{ion}}(t) = 1 - \sum_{j,K} \text{Re}(\langle \overline{\psi_{j\theta}^K} | R(\theta) | \Phi_0 \rangle^2) e^{2\text{Im}\varepsilon_j t}, \quad (10)$$

where $R(\theta)$ denotes the complex dilation operator [26], and the bar over the bra the complex conjugation in the Sturmian basis. For a detailed discussion of the action of $R(\theta)$, see reference [26]. The $|\psi_{j\theta}^K\rangle$ represent the Fourier components of the eigenstates $|\psi_{j\theta}(t)\rangle$ of \mathcal{H}_θ [26].

We can furthermore visualise the (time periodic) dynamics of the Floquet states $|\psi_j(t)\rangle$ in any representation [26] and notably in terms of the classical action angle variables I and Θ which are represented by the coherent states $|I \Theta\rangle$ [20] homogeneously covering the entire classical phase space. In order to get an explicit expression for the projection of the Floquet state $|\psi_j(t)\rangle$ onto classical phase space, we must first choose the basis in which we perform our calculations. As it is a linear representation of the dynamical group $SO(2, 1)$ of the one dimensional Coulomb potential, which, in turn, perfectly matches the symmetry properties of the unperturbed hydrogen atom, the Sturmian basis is an excellent candidate for this purpose [27]. The explicit form of a one dimensional Sturmian function writes [28]:

$$S_n^\alpha(z) = \frac{1}{\sqrt{n}} \left(\frac{2z}{\alpha}\right) e^{-z/\alpha} L_{n-1}^{(1)}\left(\frac{2z}{\alpha}\right), \quad (11)$$

where α is the same scaling parameter we already encountered in eq. (4). If we denote by $|n\rangle$ the normalized state whose wavefunction is $S_n^\alpha(z)$, the projection of $|n\rangle$ onto a coherent state $|I \Theta\rangle$ is given by [20]

$$\langle I \Theta | n \rangle = \pi^{-1/4} \frac{e^{i(n-1)\Theta}}{\sqrt{n!(n-1)!}} I^{n-1/4} e^{-I}. \quad (12)$$

The final result for the phase space projection of a Floquet state, also known as its ‘‘Husimi-distribution’’, becomes then [12, 26]:

$$\begin{aligned} & |\langle I \Theta | \psi_p(t) \rangle|^2 = \quad (13) \\ & e^{2\text{Im}\varepsilon_p t} \pi^{-1/2} I^{3/2} e^{-2I} \times \left\{ \text{Re} \left[\sum_{n,K} \frac{\cos(n\Theta - K\omega t) I^{n-1}}{\sqrt{n!(n-1)!}} \langle \overline{\psi_{p\theta}^K} | R(\theta) | n \rangle \right]^2 \right. \\ & \left. + \text{Re} \left[\sum_{n,K} \frac{\sin(n\Theta - K\omega t) I^{n-1}}{\sqrt{n!(n-1)!}} \langle \overline{\psi_{p\theta}^K} | R(\theta) | n \rangle \right]^2 \right\}. \end{aligned}$$

3 Phase Space Projections of Floquet States

We come now to the presentation of our numerical results. In the present section, we shall directly compare quantum to classical dynamics, in the space spanned by the classical action angle variables. We shall first consider the classical principal resonance, i. e. the situation where the frequency of the driving field and the Kepler frequency of the electron on its Bohr orbit coincide. We shall treat separately the stable (driving field and Coulomb motion in phase) as well as the unstable (driving field and Coulomb motion in phase opposition) situations, this is the stable and the associated unstable classical periodic orbit. Are there Floquet states which “mimick” the corresponding stable and unstable classical orbits and what are their widths (lifetimes) in the microwave field? In a second step, to which extent are the localization properties of the electronic density in phase space correlated with the lifetime of the eigenstate?

3.1 Stable and Unstable Structures in Phase Space

In order to answer the first of the above questions, we diagonalized the dilated Floquet-Hamiltonian \mathcal{H}_θ (eq. (8)) at values of the scaled amplitude and the scaled frequency of the microwave field of $F_0 = 0.035$ and $\omega_0 = 1.304$, respectively, for $n_0 = 62$. These values correspond exactly to the experimental situation described in [5]. Fig. 1 compares the Husimi distributions of two different Floquet eigenstates with the classical Poincaré surface of section obtained for $F_0 = 0.035$ and $\omega_0 = 1.304$, at two different phases $\omega t = 0$ and $\omega t = \pi$ of the driving field.

We immediately recognize the coincidence of the eigenstate displayed in figs. 1 (c), (d) with the stable region corresponding to the principal resonance in figs. 1 (a) et (b). In fact, the representation in configuration space [29] in figure 2 shows that this Floquet state is a pure coherent state which evolves with the frequency of the driving field. It has a width ($\Gamma < 10^{-14}$ a.u.) which is insignificant with respect to the maximum precision (ca. 10^{-13} a.u.) which can be obtained in our numerical calculations and can therefore be considered as a *non-dispersive* stable wavepacket locked on the microwave field. It is thus an eigenstate of the quantum system which exactly corresponds to an elliptic structure of classical phase space and evolves according to the classical equations of motion. It provides us with a perfect example of the stabilizing effect of strong nonlinear coupling.

The identification of the second eigenstate with an invariant structure of classical phase space is less immediate at $\omega t = 0$, where the quantum density is elongated along a stochastic region which actually contains a well developed cantorus [30] only hardly distinguishable on the scales of the figure. However, the association of quantal and classical structures becomes easy at phase $\omega t = \pi$: Again, the Husimi distribution *at this phase* strongly reminds us a coherent state, now concentrated at the hyperbolic fixed point associated with the principal resonance. Its width is again negligible and also this state, which is strongly scarred [11]

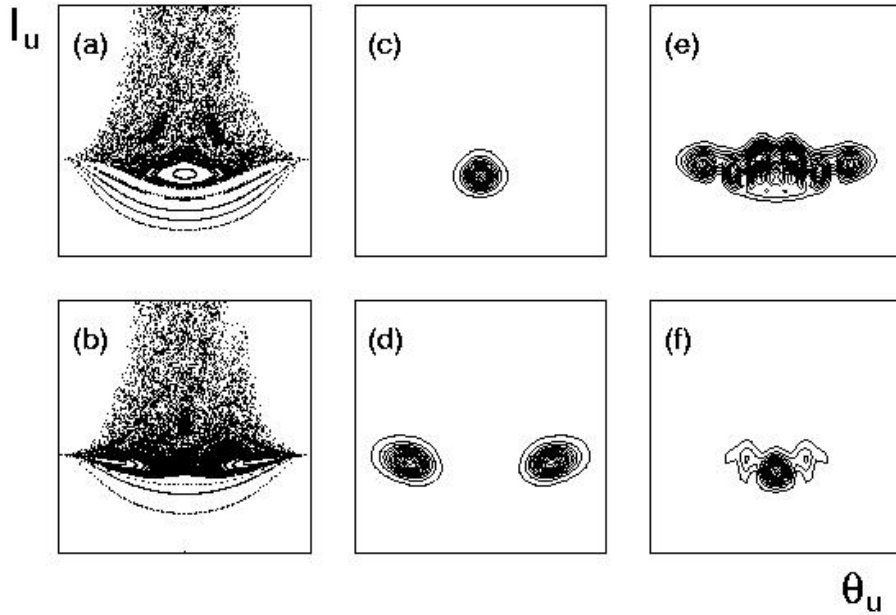


Figure 1: Comparison of the Husimi distributions ((c)-(f)) (eq. (13)) of two resonance eigenfunctions of the one dimensional hydrogen atom in a microwave field to the classical Poincaré surface of section ((a), (b)), in action angle variables (eq. (3)) $I \in [0; 160]$, $\Theta \in [-\pi; +\pi]$. Scaled angular frequency $\omega_0 = 1.304$, scaled field amplitude $F_0 = 0.035$ (for $n_0 = 62$); microwave frequency in laboratory units $\omega/2\pi = 36.02$ GHz (as in the experiments of ref. [5]). The surface of section as well as the Husimi distributions are presented for two different values of the phase of the driving field. Upper row: $\omega t = 0$; lower row: $\omega t = \pi$. The eigenstate represented in (c) and (d) clearly follows the principal resonance in the classical phase space. The eigenstate represented in (e) and (f) is rather concentrated in the stochastic region close but outside the principal resonance; at phase $\omega t = \pi$ it comes close to a coherent state concentrated at the hyperbolic fixed point associated with the principal resonance; it's a scar [11]. *Both* quantum states have very long lifetimes and thus nondispersive character, despite the very different stability properties of the associated classical trajectories.

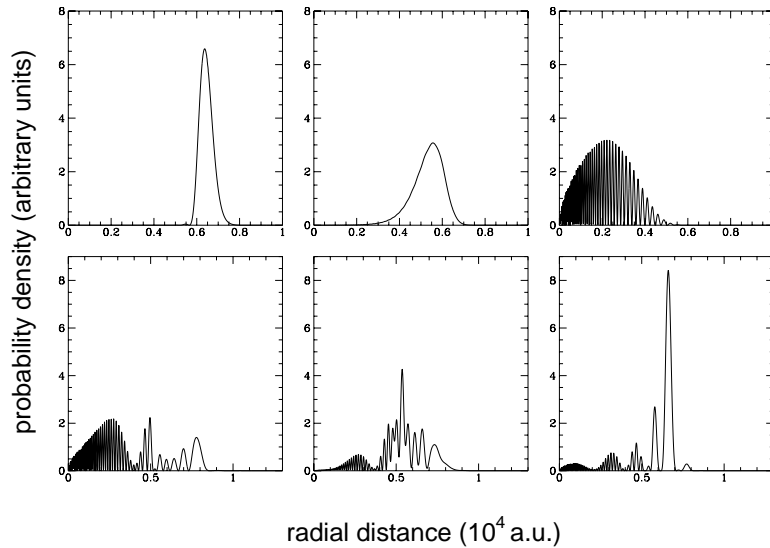


Figure 2: Configuration space representation of the resonance eigenfunctions projected onto the classical phase space in fig. 1. The states evolve in time with the periodicity of the external microwave field. We show the wavepackets at phases $0, \pi/2$ and π (from left to right). Top: When the classical motion is regular, the quantum wavepacket is localized in phase space, locked on the external frequency and *non dispersive*. This corresponds to the Husimi distribution of fig. 1 (c) and (d). Bottom: When the classical motion is chaotic, the quantum wavepacket may be partially localized on complex phase space structures, with a quasi-random background. This corresponds to the Husimi distribution of fig. 1 (e) and (f). Note the phase difference of π between the regular and chaotic wavepackets.

along an unstable periodic orbit, has a nondispersive stable character. Recall, however, that, at a hyperbolic point, a contracting and an expanding direction of the classical probability flux cross [4]. In order to ensure the periodicity of the Floquet states, we *cannot* find but a coherent state polluted by contributions corresponding to the outgoing and ingoing directions of the classical flux, the latter ones refeeding the losses introduced by the former. The representation of the same eigenstate in configuration space (see fig. 2) shows indeed that these pollutions induce an interference pattern and that we do not face here a coherent state as above [29]. A complementary observation has recently been made in the study of the dynamics of a coherent state initially placed on a hyperbolic fixed point of the piecewise linear map [31, 32, 33].

3.2 Localisation and Lifetimes

In the preceding section, we have given two examples for the concentration of the electronic densities of Floquet eigenstates of the microwave problem along classical periodic (stable and unstable) orbits, a phenomenon which already has been observed by other authors [10]. We found in both cases that the eigenfunctions had a very long lifetime in the microwave field, largely longer than typical experimental interaction times which correspond to resonance widths of the order of $\Gamma \simeq 2.8 \times 10^{-10}$ a.u. [34]. Whereas this may seem natural for the eigenstate associated with the classically stable structure (figs. 1 (c), (d)), it may be more surprising for the scarred state localized along the unstable periodic orbit which one would classically expect to diffuse in phase space and finally ionize, on a relatively short time scale. It has been argued [11] that scars have a stabilizing effect on the quantum dynamics and that the stability of the state we plotted in figs. 1 (e) and (f) is due to its strong localization along the classical action. However, fig. 3 shows that the localization properties of a Floquet state in phase space are not a sufficient criterion for the prediction of its lifetime in the microwave field. There are states which are strongly delocalized (fig. 3 (b)) in phase space with a smaller width ($\Gamma \simeq 3.6 \times 10^{-11}$ a.u.) than eigenstates which are apparently strongly localized close to the principal resonance (fig. 3 (c)) but with a larger width ($\Gamma \simeq 1.6 \times 10^{-10}$ a.u.) [35]. Analyzing a complete Floquet spectrum for the abovementioned values of the microwave frequency and amplitude shows that there is certainly a correlation between the lifetime of an eigenstate and the localisation properties of the electronic density in action angle variables, but that this correlation, hence, permits only statistical predictions. The localization of the electronic density in phase space will certainly favour longer lifetimes, but there are nonetheless strong fluctuations of the latter around the statistical mean value which prevent from the prediction of the lifetime of an individual eigenstate. Consequently, the identification of a scarred wavefunction [11] as being at the origin of an experimentally observed, local stability of the atom with respect to its ionization by the microwave [5] only on the grounds of its localization prop-

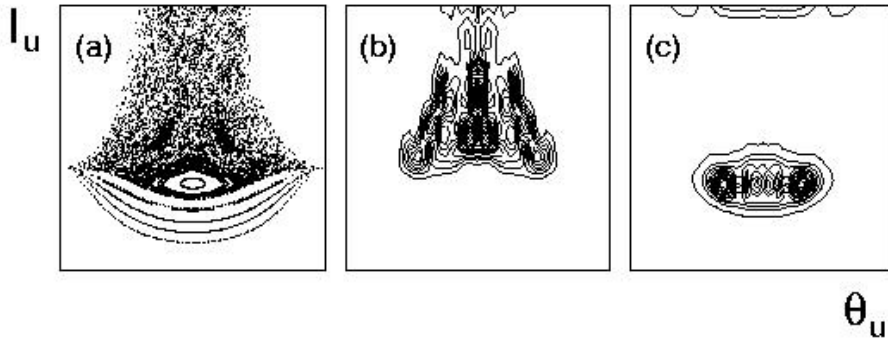


Figure 3: Husimi distributions of two different resonance eigenstates which are strongly delocalized (b) and strongly localized (c) in the classical phase space (a) (with $F_0 = 0.035$, $\omega_0 = 1.304$, $\omega/2\pi = 36.02$ GHz). Width of the resonance in (b): $\Gamma \simeq 3.6 \times 10^{-11}$ a.u.; and in (c): $\Gamma \simeq 1.6 \times 10^{-10}$ a.u. the more localized wavefunction has the shorter lifetime, contrary to the statistically prevailing correlation of strong localization and weak decay to the continuum.

erties, is *not* convincing. Recall that the typical interaction and thus ionization times in current microwave experiments on hydrogen [34] correspond to about 200 passages of the unperturbed Kepler electron close to the nucleus. This means that it must be the asymptotic properties of the electronic density, i. e. its distribution at small amplitudes *far* from the initial state which determine the ionization behaviour, rather than the distribution in the neighbourhood of the initially prepared state. The observed correlation of local and asymptotic aspects shows that both aspects are related, however *not* in a systematic manner.

Let us also mention that we have no indication which would attribute any significance to the scarring phenomenon as far as the stabilization of an atom with respect to ionization by the driving field is concerned. There are Floquet states which are concentrated along elliptic or along unstable regions, others show both aspects simultaneously, without any systematic trend in the corresponding lifetimes. A study [12] of the level dynamics and the evolution of the corresponding eigenstates from the weak field to the intense field limit rather suggests the association of the stable scarred wavefunction of figs. 1 (e), (f) with a cantorus and thus with an object clearly originating from a stable classical structure. Such a picture would rather support the older semiclassical idea of the inhibition of quantum transport by partial barriers in classical phase space which are less permeable for quantum than for classical probability flux [36, 37]. Obviously, Floquet states associated with such “vague tori” or “cantori” [30, 38] imply the population of unstable regions of phase space (as a consequence of the finite size of \hbar), without allowing for a neat isolation of an individual scar and the associated unstable periodic orbit at the origin of the local stability. This is not too surprising as we

are dealing here with a typically mixed phase space, whereas the concept of scars has been developed in the context of globally chaotic dynamics [39].

4 Quasienergies and Ionization Probabilities

After our study of some individual eigenstates of the Floquet spectrum, together with their widths and phase space projections, we will now try to understand how the spectral properties of our system manifest themselves in the ionization probability P_{ion} of an atom initially prepared in a state n_0 .

The ionization probability as a function of the microwave amplitude, for all the other experimental parameters (initial atomic state n_0 , microwave frequency $\omega/2\pi$ and interaction time t) fixed, is actually the basic unit of all current laboratory experiments on the microwave ionization of Rydberg states [5, 6, 7]. It can be directly calculated from the imaginary parts of the eigenvalues and from the eigenvectors of \mathcal{H}_θ , according to eq. (10). The field amplitude at which the ionization probability takes a value of 10% defines the so-called “(10%) ionization threshold field” $F_0(10\%)$ and can finally be represented in its dependence on the experimental parameters which are left (initial atomic state, microwave frequency and interaction time) [5, 6, 7]. This definition tacitly implies an essentially monotonous behaviour of P_{ion} with F , an assumption which is not always true and may lead to a certain ambiguity of the experimental results, as far as local structures of $F_0(10\%)$ vs. the free parameters n_0, ω, t are concerned [5, 17, 40].

Fig. 4 shows the ionization probability of the state $|n_0 = 23\rangle$ as a function of the microwave amplitude, at two different values of the scaled angular frequency $\omega_0 = 1.0$ and $\omega_0 = 1.18$. We observe a locally non-monotonous behaviour (“subthreshold peaks”) of the ionization signal P_{ion} in both cases, at certain values of F , together with an increase of P_{ion} with F , in the average. Both curves are opposed to the level dynamics of the associated real and imaginary parts of the Floquet states generating the dynamics, and it is easy to identify the (anti-) crossings of the (real) imaginary parts of the complex quasienergies $\varepsilon_{j\theta}$ at the origin of the non-monotonies of the ionization signal [41]. The dashed lines in figs. 4 (a) and (d) indicate an ionization probability of 10%, whereas they mark the imaginary part of the complex quasienergy $\varepsilon_{j\theta}$ which corresponds to an ionization yield of 10% during the chosen interaction time, in figs. 4 (b) and (e). Note that those anticrossings which induce the subthreshold peaks are almost unresolved in the real energy levels, whereas they correspond to very prominent structures in the dynamics of the imaginary parts of the quasienergies (which are plotted on a logarithmic scale!). Apart from the energy levels which exhibit (anti-) crossings in their complex resonance spectrum, there are also energy levels which pass smoothly and without notable interaction with other states through the entire intervall of the microwave amplitude we have chosen. They give rise to the global increase of P_{ion} with F , which is locally altered by the anticrossing

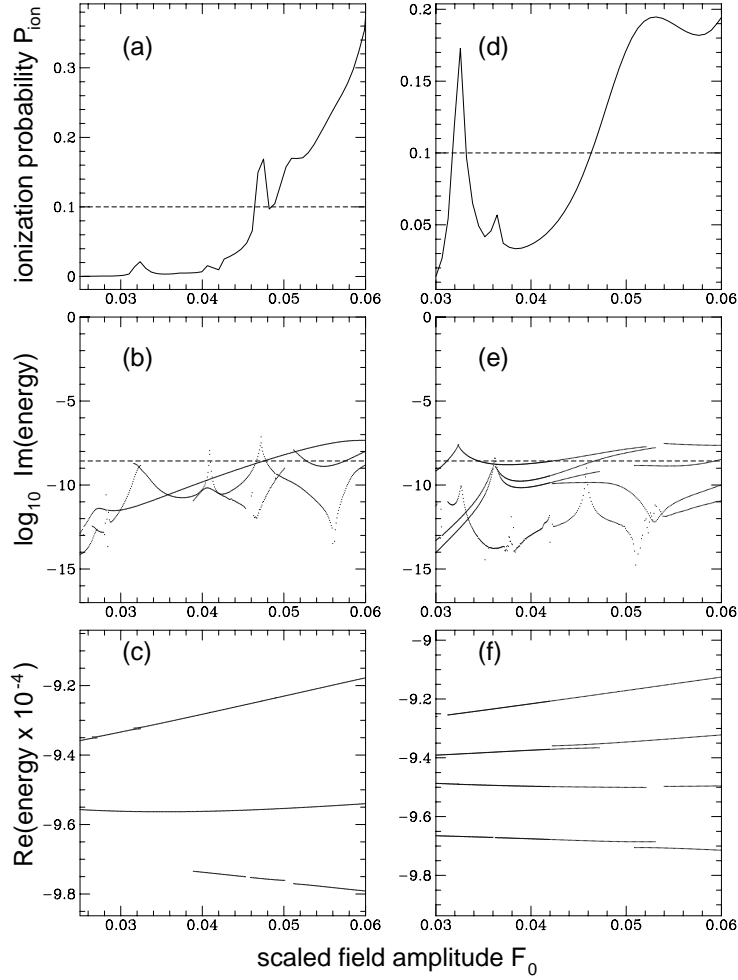


Figure 4: Ionization probabilities (top) of the state $|n_0 = 23\rangle$ exposed to a microwave field, opposed to the imaginary (middle) and the real parts (bottom) of the resonance eigenvalues of the eigenstates dominating the ionization process, as a function of the scaled microwave amplitude, and for two different values of the scaled frequency of the driving field. (a)-(c): $\omega_0 = 1.0$; (d)-(f): $\omega_0 = 1.18$. Microwave interaction time: $t = 4.6 \times 10^{-10}$ s. Note the sharp subthreshold peaks in (a) and (d), and the corresponding locally sharp increase of the imaginary parts of individual resonance eigenvalues at exactly the same values of F_0 . These crossings of the imaginary parts correspond to avoided crossings of the resonance energies (in (c) and (d)) which are almost unresolved on the scales of the figure. One also observes that the broad local maximum of the ionization signal in (d) ($F_0 \simeq 0.053$) corresponds to the locally smooth and simultaneous increase of a few widths in (e). In all the Floquet spectra shown in the present and in the following figures, only those eigenvalues are taken into account which correspond to eigenstates with an overlap of more than 5% to 10% with the initial state the atoms are prepared in (see eq. (10) and [41]).

Floquet states. Another phenomenon is observed in figs. 4 (d)-(f): apart from isolated (avoided) crossings which induce a narrow subthreshold structure, there are several energy levels which simultaneously increase their widths, before decreasing again to smaller values. The result is a relatively broad “shoulder” in the ionization signal.

How does the position of the small and isolated avoided crossings giving rise to the sharp subthreshold peaks observed above depend on the frequency of the driving field and on the initial state of the atoms? Fig. 5 shows the level dynamics of the imaginary parts of the $\varepsilon_{j\theta}$ on the same interval as in fig. 4, for six different values of ω_0 in the vicinity of 1.300. Whereas the global aspect does not change considerably, we see that there are some crossings and nonmonotonous structures of the imaginary parts of the quasienergies, the positions of which move quite considerably (by ca. $\Delta F \simeq 0.01$) for a change of ω_0 by only $\delta\omega_0 \simeq 0.005$. It is only on a scale of $\delta\omega_0/\omega_0 \simeq 1 \times 10^{-3}$ that a continuous motion of these structures with ω_0 can be observed, they cannot be tracked any more for larger changes in the frequency! Hence, the position of the associated subthreshold peaks in the ionization signal will in principle be *extremely* sensitive with respect to changes in the frequency of the driving field [42, 43, 44]. However, a similar analysis of the dependence of the position of the (avoided) crossings and potential subthreshold structures on the value of the principal quantum number leads to a different result: as the properties of the Floquet spectrum do not depend on the initial value of n_0 , it is only the change of the projection of the initial state onto the Floquet states which changes the ionization signal and eventual subthreshold structures. This projection being a smooth function of n_0 (a typical Floquet eigenstate spreads over several consecutive n states [17]), also the subthreshold peaks in the ionization signal evolve slowly. Hence, the sensitivity of the subthreshold peaks with respect to changes in the physical frequency is a pure quantum phenomenon which *cannot* scale classically! It transposes the sensitive dependence on the initial conditions of a classical irregular system to the sensitive dependence of the quantum analogue with respect to changes in the external parameters. This phenomenon has also been observed in the numerical study of other (quantum) chaotic systems [29] and may possibly be considered as a defining property of quantum chaos. It should be also noted that the sensitive dependence of the position of the subthreshold peaks may be an indication for the existence of the so-called “universal conductance fluctuations” [42] also in the microwave domain [42, 43, 44]. This feature of mesoscopic solid state samples consists in erratic changes of the conductance when the parameters defining the precise physical conditions are only slightly changed. Since the problem of charge transport in a one dimensional sample can be formally identified with the energy exchange between a Rydberg electron and a microwave field (restricted to one spatial dimension and neglecting the finite widths of the Floquet states induced by the continuum coupling) [45], the conductance fluctuations in the solid state sample have been expected to manifest themselves as fluctuations in the ioniza-

tion probability of the Rydberg state [42], i. e. in the properties of the energy transport along the Rydberg series. As we shall see in the next paragraph in more detail, the conditions for the experimental observation of “conductance fluctuations” in the microwave excitation of Rydberg states may, however, be quite restrictive with respect to the interaction time of the atoms with the microwave, as well as with respect to the envelope of the microwave pulse seen by the atoms. The rise time of the latter should be shorter than the time needed to resolve the width of the associated anticrossing, the former should be chosen such that the global ionization yield from all the eigenstates involved in the ionization process is small, apart from the contribution of the states interacting at the anticrossing.

The material we are presenting here for the microwave problem is certainly not yet complete, and the investigation of the sensitivity versus changes in the field amplitude, at fixed frequency, is yet lacking. However, we expect just the same qualitative result.

5 Quasienergies and Time-scales

We have seen in the previous paragraph that the experimentally observed ionization signal is marked by local as well as by global aspects of the level dynamics of the resonance eigenvalues. Since $P_{\text{ion}}(t)$ is a function of the imaginary part of the $\varepsilon_{j\theta}$, it immediately follows that these aspects will introduce at least two different time scales in our problem. Let us first consider the time scale associated with the local structures of the spectrum.

5.1 “Local” Time-scales

Local structures in the resonance spectrum of the microwave problem, such as isolated (avoided) crossings of the (real) imaginary parts of the resonance eigenvalues, may induce local structures in the ionization signal which is at the very basis of most current experimental approaches. However, those local structures do typically appear within a finite interval of the imaginary part of the resonance eigenvalues which corresponds to a finite interval of the experimental interaction time. For longer interaction times, the associated eigenstates do no more contribute to the ionization dynamics, they already are ionized. For shorter interaction times, these eigenstates do not yet contribute considerably to the ionization yield and the experiment is therefore not able to probe the local properties of the spectrum. Hence, the appearance of subthreshold peaks, as well as their sensitivity versus changes of an external parameter is a *transient* phenomenon, restricted to a possibly narrow window in the interaction time!

Fig. 6 illustrates this remark, as it shows the ionization signal of the state $|n_0 = 62\rangle$ exposed to a microwave field of scaled frequency $\omega_0 = 1.304$, for three different values of the interaction time which differ by at most a factor of

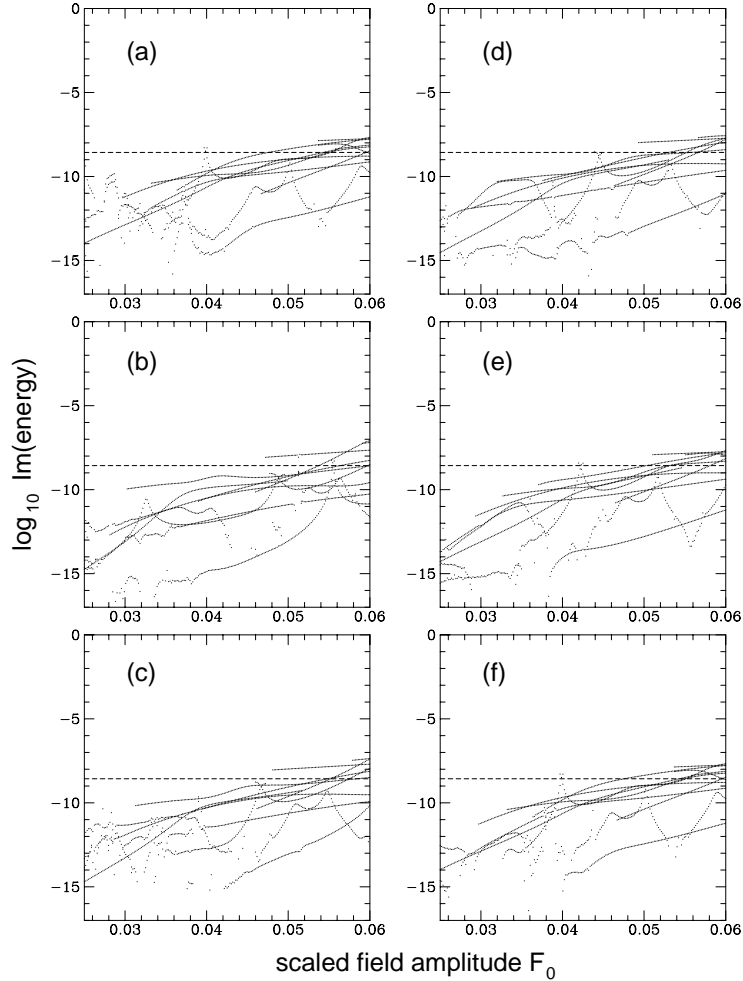


Figure 5: Level dynamics of the imaginary parts of the resonance eigenvalues of the eigenstates dominating the ionization of the state $|n_0 = 23\rangle$ by a microwave field, for different nearby values of the scaled angular frequency of the microwave, at $n_0 = 23$ fixed. $\omega_0 =$ (a) 1.300, (b) 1.301, (c) 1.302, (d) 1.303, (e) 1.304, (f) 1.305. Whereas the global behaviour is essentially unaffected by the changes in the frequency, we observe a considerable motion of the nonmonotonous local structures (which are at the origin of the subthreshold peaks of fig. 4) with ω .

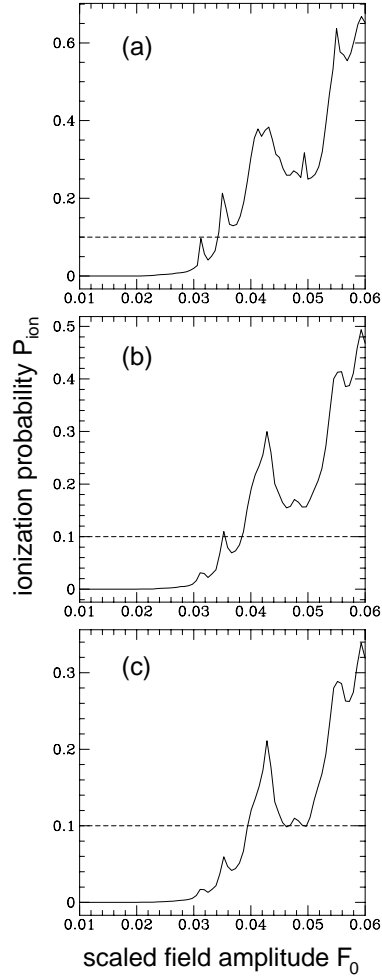


Figure 6: Ionisation signal of the state $|n_0 = 62\rangle$ in a microwave field of scaled angular frequency $\omega_0 = 1.304$, for different values of the interaction time $t =$ (a) 9.1×10^{-9} s, (b) 3.7×10^{-9} s, (c) 1.9×10^{-9} s. Note how the subthreshold structure (respectively the consecutive *decrease* in the ionization probability) emerge from the globally increasing ionization signal when the interaction time is shortened. This results in a considerable difference of the ionization threshold field of more than 20% for a change of the interaction time by a factor 2 to 5.

roughly 4.5. Note how the change in the interaction time supplies the isolated avoided crossing at $F_0 \simeq 0.041$, and hence the associated subthreshold peak clearly distinguishable in part (b) and (c) of figure 6, with a bigger relative contribution to the ionization signal the shorter the interaction time. Shortening the interaction time does not only favour the emergence of the nonmonotony of P_{ion} , but also changes the ionization threshold field, as we can see from the comparison of 6 (b) to 6 (c), by a considerable value of about $\Delta F_0(10\%) \simeq 0.01$ (which is ca. 20%!). This observation shows that one has to be *extremely* careful when changing free parameters in a (1d) numerical simulation of the microwave ionization of Rydberg states [10, 28]. Recall that all the local structures generally observed in laboratory or numerical experiments are only small corrections to the global behaviour.

Let us finally evoke once more the quantum origin of the subthreshold peaks: increasing the microwave amplitude increases the multiphoton transition amplitudes to the continuum at any order of the ionization process. Hence, a *decrease* of the ionization probability (subsequent to a subthreshold peak) with *increasing field strength must* be due to the *destructive interference* of transition amplitudes at different orders. This underlines as well the purely quantal as the highly nonlinear or nonperturbative origin of the observed phenomenon and of the associated time-scales.

5.2 “Global” Time-scales

We just have seen how local structures of the Floquet spectrum may induce relatively short time scales on the experimentally observed ionization probability. However, apart from the dynamics of an individual quasienergy-level with rising field amplitude, there is also a collective, average “motion” of the levels towards larger values of the imaginary parts of the resonance eigenvalues. This introduces a time scale which generically encompasses several orders of magnitude and which can be tested by the time dependence of the ionization threshold field, at fixed values of frequency and initial state [7, 46]. Fig. 7 shows the result of a numerical simulation of the time dependence of $F_0(10\%)$ for $n_0 = 23$, over four orders of magnitude of the interaction time t . We observe an almost algebraic decay $F_0(10\%) \propto t^{-\gamma}$ of the ionization threshold field with an exponent $\gamma \simeq 0.07$. Recall that a perturbative approach yields $\gamma_{\text{pert}} = 1/2N$, for a N -photon transition to the continuum. With $n_0 = 23$ and $\omega_0 \simeq 1.6$ we actually find $\gamma_{\text{pert}} \simeq 0.07$, the numerical result. Remarkably, however, in our numerical simulation, γ does not seem to depend strongly on the frequency of the driving field, since the figure shows results for ω_0 ranging from $\omega_0 = 0.8$ to $\omega_0 = 3.0$. γ_{pert} should then vary between ca. $\gamma_{\text{pert}} \simeq 0.04$ and $\gamma_{\text{pert}} \simeq 0.14$, values which are distinct from the numerical results. Hence, also the present time-scale seems rather of non-perturbative origin.

Let us finally mention that we observed larger values of γ (up to $\gamma = 0.2$) in

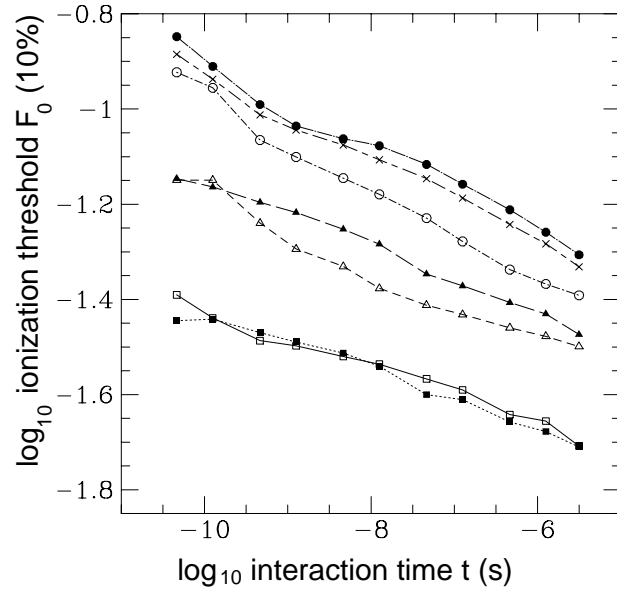


Figure 7: Time dependence of the scaled 10% ionization threshold of the state $|n_0 = 23\rangle$ in a microwave field of scaled frequency ω_0 . Open squares: $\omega_0 = 0.608$, filled squares: $\omega_0 = 0.8$, open triangles: $\omega_0 = 1.3$, closed triangles: $\omega_0 = 1.43$, open circles: $\omega_0 = 2.0$, filled circles: $\omega_0 = 2.7$, crosses: $\omega_0 = 3.0$. The algebraic decay $F_0(10\%) \propto t^{-\gamma}$ over four orders of magnitude of the interaction time is obvious. The exponent $\gamma \simeq 0.07$ is essentially unaffected by changes of the frequency.

the immediate vicinity of ω_0 ($\omega_0 \simeq 2.44 \dots 2.6$), with some deviations from the monoalgebraic decay which are introduced by subthreshold peaks in the ionization signal. The origin of this phenomenon has not been clarified up to now.

6 Conclusion

In conclusion, we provided a detailed picture of the interplay of local and global aspects of the resonance spectrum of a hydrogen atom exposed to a microwave field and of the impact on experimentally accessible quantities as ionization probabilities and threshold fields. We investigated individual eigenstates in their representation in action angle space, their localization properties and their widths induced by the microwave interaction. We have seen that scarring is an ubiquitous phenomenon experienced by a lot of Floquet eigenstates, but that it has - in itself - no relevance for the analysis of local structures of the ionization threshold as a function of the frequency of the microwave. We also illustrated how isolated avoided crossings can produce subthreshold peaks in the ionisation signal, provided the experimental interaction time is compatible with the typical time scale associated with the individual crossing. We furthermore observed that the positions of the anticrossings in the resonance spectrum depend very sensitively on changes of the frequency of the driving field, a typical signature of quantum chaos and possibly of “universal conductance fluctuations” in the microwave problem. We finally observed the existence of a second time scale being due to the global dynamics of the energy levels with the perturbation strength, and well separated from the time scales typically induced by avoided crossings.

Acknowledgements

We are grateful to Giulio Casati and Giorgio Mantica for the invitation to the E.S.F. Workshop on Classical Mechanical Methods in Quantum Mechanics in Como, Italy, May 15 to July 15, where part of this work has been accomplished. A.B. should like to thank Bala Sundaram for helpful discussions at Como, and the European Community for financial support through the “Science” program. CPU time on a CRAY-2 and a CRAY-YMP-EL computer has been provided by the Conseil Scientifique du Centre de Calcul Vectoriel pour la Recherche and by the Centre de Calcul pour la Recherche de l’Université Pierre et Marie Curie, respectively. Laboratoire de Spectroscopie Hertzienne de l’Ecole Normale Supérieure et de l’Université Pierre et Marie Curie is Unité Associée 18 du Centre National de la Recherche Scientifique.

References

- [1] Iu C. H., Welch G. R., Kash M. M., Kleppner D., Delande D., Gay J. C., Phys. Rev. Lett. **66**, 145 (1991).
- [2] G. Raithel, M. Fauth, and H. Walther, Phys. Rev. **A44**, 1898 (1991).
- [3] K. Richter, J. S. Briggs, D. Wintgen and E. A. Solov'ev, J. Phys. **B25**, 3929 (1992).
- [4] A. J. Liebermann, M. A. Lichtenberg, *Irregular and Stochastic Motion*, Applied Mathematical Series, Vol. 38, Springer-Verlag, New York 1983.
- [5] B. E. Sauer, M. R. W. Bellermaun, and P. M. Koch, Phys. Rev. Lett. **68**, 1633 (1992).
- [6] J. E. Bayfield and D. W. Sokol, Phys. Rev. Lett. **61**, 2007 (1988).
- [7] M. Arndt, A. Buchleitner, R. N. Mantegna, and H. Walther, Phys. Rev. Lett. **67**, 2435 (1991).
- [8] J. E. Bayfield and D. W. Sokol, *Highly excited hydrogen atoms in strong microwaves*, in: Physics of Atoms and Molecules: Atomic Spectra and Collisions in External Fields. edited by K. T. Taylor, M. H. Nayfeh, C. W. Clark, Plenum Press, New York 1988.
- [9] R. Blümel, A. Buchleitner, R. Graham, L. Sirko, U. Smilansky, H. Walther, Phys. Rev. **A44**, 4521 (1991).
- [10] R. V. Jensen, S. M. Susskind, and M. M. Sanders, Phys. Rep. **201**, 1 (1991).
- [11] R. V. Jensen and M. M. Sanders, M. Saraceno, B. Sundaram, Phys. Rev. Lett. **63**, 2771 (1989).
- [12] A. Buchleitner, thèse de doctorat, Paris 1993.
- [13] G. Casati and B. V. Chirikov, I. Guarneri, and D. L. Shepelyansky, Phys. Rev. Lett. **59**, 2927 (1987).
- [14] G. Casati, I. Guarneri, D. L. Shepelyansky, IEEE J. Quantum Electron. **24**, 1420 (1988).
- [15] A. Buchleitner and D. Delande, Phys. Rev. Lett. **70**, 33 (1993).
- [16] A. Buchleitner and D. Delande, in preparation.
- [17] A. Buchleitner, D. Delande, and J. C. Gay, submitted to J. Opt. Soc. Am. **B**, 1994.

- [18] M. Nauenberg, *Europhys. Lett.* **13**, 611 (1990).
- [19] J. Zakrzewski, D. Delande, and J. C. Gay, K. Rzażewski, *Phys. Rev.* **A47**, R2468 (1993).
- [20] D. Delande, *Atomes de Rydberg en champs statiques intenses*, Thèse de Doctorat d'état, Université Pierre et Marie Curie, Paris 1988.
- [21] G. Floquet, *Ann. École Norm. Sup.* **12**, 47 (1883).
- [22] J. H. Shirley, *Phys. Rev.* **138**, B979 (1965).
- [23] H. P. Breuer, K. Dietz, et M. Holthaus, *Z. Phys.* **D8**, 349 (1988).
- [24] K. Yajima, *Comm. Math. Phys.* **87**, 331 (1982).
- [25] S. Graffi et al., *Ann. Inst. H. Poincaré* **42**, 215 (1985).
- [26] A. Buchleitner, B. Grémaud, and D. Delande, submitted to *J. Phys.* **B**, 1994.
- [27] D. Delande and J. C. Gay, *J. Phys.* **B17**, L335 (1984).
- [28] R. Blümel and U. Smilansky, *Z. Phys.* **D6**, 83 (1987).
- [29] D. Delande and A. Buchleitner, to be published in *Adv. At. Mol. Opt. Phys.*, 1994.
- [30] I. Percival, *Recent developments in classical mechanics*, in: *Les Houches école d'été de physique théorique, session LII*, edited by M.-J. Giannoni, A. Voros et J. Zinn-Justin, North-Holland, Amsterdam, 1991.
- [31] R. Scharf and B. Sundaram, *Phys. Rev.* **A45**, 3615 (1992).
- [32] R. Scharf and B. Sundaram, *Phys. Rev.* **A46**, 3164 (1992).
- [33] R. Scharf and B. Sundaram, oral contribution on the E.S.F. Workshop on Classical Mechanical Methods in Quantum Mechanics, May 15 to July 15, 1993, Como, Italy.
- [34] D. Richards, J. G. Leopold, P. M. Koch, E. J. Galvez, K. A. H. v. Leeuwen, L. Moorman, B. E. Sauer and R. V. Jensen, *J. Phys.* **B22**, 1307 (1989).
- [35] The non-vanishing amplitudes of the electronic density at the upper edge (maximum value of I) of the Husimi distributions are traces of the “continuum contributions” to each individual resonance [26]. They determine the continuum coupling and thus the width of the state but have *no* significance as a bound space projection. That they become visible at finite values of the classical action simply expresses the fact that the diagonalisation of our eigenvalue problem has been effectuated using a truncated basis of the Hilbert space [17].

- [36] G. Radons, T. Geisel, J. Rubner, *Classical chaos versus quantum dynamics: KAM tori and cantori as dynamical barriers*, in: Lasers, Molecules and Methods, edited by J. O. Hirschfelder, R. E. Wyatt and R. D. Coalson, Wiley, 1989.
- [37] O. Bohigas, S. Tomsovic, and D. Ullmo, Phys. Rep. **223**, 43 (1993).
- [38] R. B. Shirts and W. P. Reinhardt, J. Chem. Phys. **77**, 5204 (1982).
- [39] E. J. Heller, *Wavepacket dynamics and quantum chaology*, in: Les Houches école d'été de physique théorique, session LII, edited by M.-J. Giannoni, A. Voros et J. Zinn-Justin, North-Holland, Amsterdam, 1991.
- [40] R. Blümel, U. Smilansky, J. Opt. Soc. Am. **B7**, 664 (1990).
- [41] In all the Floquet spectra we show in the present paper, only those eigenvalues are taken into account which correspond to eigenstates with an overlap of more than 5% to 10% with the initial state the atoms are prepared in (see eq. (10)). This selects the few states which contribute significantly to the ionization probability (eq. (10)) within the several hundred eigenstates of a typical numerically obtained Floquet spectrum. As the overlap with the initial state is a function of the field strength, too, some of the energy levels represented in the level dynamics show interruptions.
- [42] G. Casati, I. Guarneri, and D. L. Shepelyansky, Physica **A163**, 205 (1990).
- [43] J. G. Leopold and D. R. Richards, J. Phys. **B23**, 2911 (1990).
- [44] J. G. Leopold and D. R. Richards, J. Phys. **B24**, 1209 (1991).
- [45] D. R. Grempel and R. E. Prange, S. Fishman, Phys. Rev. **A29**, 1639 (1984).
- [46] S. Fishman and D. L. Shepelyansky, Europhys. Lett. **16**, 643 (1991).